ELSEVIER

Biophysical Chemistry 74 (1998) 23–34

Biophysical Chemistry

Study of α-helix to β-strand to β-sheet transitions in amyloid: the role of segregated hydrophobic β-strands

Saul G. Jacchieri*

Fundação Antônio Prudente, Rua Prof. Antônio Prudente 211, Sao Paulo, SP 01509-900, Brazil

Received 8 September 1997; received in revised form 17 March 1998; accepted 23 April 1998

Abstract

A conformational analysis including three polypeptide chains known to be amyloidogenic and neurotoxic has shown the occurrence of low probability hydrophobic β-strands stabilized by intramolecular interactions. It is argued that by engaging in non-bonded and hydrophobic interactions these β-strands seed the assembly of β-sheets in amyloid fibrils following a non-cooperative mechanism dissimilar to β-sheet folding in proteins. Molecular models of amyloid fibrils formed by such β-strand templates were built. It is shown that the parallel alignment of β-strands creates an extensive hydrophobic surface whereas the antiparallel alignment causes the formation of hydrophobic and hydrophilic aggregates. A comparison with experimental data and previous calculations is established.

Keywords: Amyloid fibril; Non-cooperative aggregation; Segregated β-strands

1. Introduction

Transitions from α-helix to β-sheet (α/β transition), two major secondary structural motifs of protein structure [1], are known [2] to be associated with degenerative diseases of nervous tissues such as Alzheimer, Creutzfeldt-Jakob and Scrapie. An event common to these and other neurodegenerative diseases is the formation of β-sheet aggregates known as amyloid plaques [3] which, among other features, are extremely resistant to protease action, an indication of close packed clusters. It is a general observation that solubility and protease resistance depend on actual secondary structure. α-Helical and/or random coil content has been shown to be coincident with high solubility [4] and protease susceptibility [2] whereas a β-sheet content has been shown to determine poor solubility [4] and resistance to proteolysis [2].

Such structural transitions have been observed in a variety of protein and peptide chains that includes different strains of the PrP^{SC} protein [5],

* Fax: +55 11 2425088.

0301-4622/98/$19.00
PII S0301-4622(98)00157-4

the β-amyloid protein [6], lysozyme [7] and transthyretin [8] mutants. Recently, experimental models [9] of the α/β transition have also been designed which, besides being models of amyloid formation, are also useful for understanding protein folding mechanisms.

In the present study we have undertaken a conformational analysis of the cellular prion protein (PrP^C) peptides 106–126, 114–129 and 114–133, listed in Table 1. Studies [10] that probed the amyloidogenic potential and neurotoxicity of peptides derived from non-contiguous regions of PrP^C have shown that the peptide chains 109–122, 113–127, 178–191 and 202–218 are amyloidogenic. The latter two peptide chains are not homologous to each other or the former two, indicating that amyloid formation may proceed through non-related mechanisms. However, it has also been shown [11] that peptides belonging to the same region of peptides 109–122 and 113–127 (which have been predicted to be α-helical) are neurotoxic. Furthermore, this domain is the most conserved through evolution [11].

Theoretical models of α/β transitions in amyloidogenic peptides should explain the susceptibility to formation of β-sheet clusters among various polypeptide chains as well as different chain regions. Another important question is whether the mechanism of β-sheet folding is the same in proteins and amyloid fibrils.

We have made use of methods previously employed in the study of other structural transitions, such as the helix-coil transition [12], a characterization of possible α-MSH structural transitions [13] from aqueous solution to membrane bound conformations and, more recently, peptide chain structural transitions related to oligopeptidase specificity for conformation [14].

2. Theory

2.1. Conformational analysis

Part of the present study was carried out with matrix operations [12]. The calculations include the generation of matrices of statistical weights dimensioned in accordance with the numbers of main chain and side chain conformers considered appropriate and interaction ranges spanning the most important interactions. By taking advantage of a feature of the matrix algorithm [12] that makes it possible to freeze part of the chain in a certain conformation, we have allowed three conformers to each side chain (for alanine and glycine one side chain conformer was considered), five conformers to the main chain of each amino acid residue and an interaction range spanning the whole chain.

The process is outlined here and described in detail in the theory section of ref. [14]. The initial step is the generation of a set of conformations for the tetramer fragment closer to the amino end.

$$M_4 = M_1 \otimes O_2 \otimes O_3 \otimes O_4 \quad (1)$$

where the matrices M of statistical weights and O of exponential factors formed by interaction energies are described in ref. [12].

The conformations generated by Eq. (1) are then sorted in order of increasing energies. A set of S conformations belonging to the most stable 40 kcal/mol interval is selected with a criterion [14] that discriminates those conformations belonging to maxima and minima in density of states [15,16] vs. energy plots.

In the next cycle the product

$$M_4 = M_1 \otimes O_2 \otimes O_3 \cdots \otimes O_8 \quad (2)$$

is repeated S times so that the chain fragment 1–4 may be kept frozen in each of the S conformations previously selected. The process is continued until the end of the chain. This methodology has some similarities to the build up procedure [17]. The main significant differences are the use of a density-of-states-based criterion to sample chain conformations in each cycle and the adoption of a matrix algorithm.

The result of this conformational search is a set of chain conformations sorted in increasing energy order. Since strings of main chain (represented by letters) and side chain (represented by numerals) rotamers define chain conformations [12] it is possible [18] to search a structural motif in the set by comparing strings. A set of chain

conformations adopting the same structural motif may then be obtained. Energy distributions [15] such as those shown in Fig. 2 are obtained from these sets.

2.2. Cooperativity versus non-cooperativity

The argument developed in this manuscript is concerned with the cooperativity (and possible non-cooperativity) of the protein folding process.

β-Pleated sheet folding is intrinsically a cooperative process, since it requires the immobilization of the main chain dihedrals belonging to the β-strand that seeds the structure. Nonetheless, α-helix folding is also a cooperative process that may turn out non-cooperative for alanine based sequences [19].

One may argue whether there are sequences that cause a non-cooperative β-sheet folding. Considering that a sequential positioning of β-strand- turn- β-strand... chain regions may be required for the formation of an antiparallel pleated sheet we conclude that if, for instance, a β-strand has six amino acid residues and a reverse turn has four a total of 20 main chain dihedral angles is constrained when a folding unit is formed, without a net enthalpy gain. Adding two β-strands to both sides of the growing sheet causes the formation of 12 hydrogen bonds.

On the other hand, six dihedral angles are constrained in α-helix nucleation to form one hydrogen bond, whereas elongation requires the immobilization of two dihedral angles per hydrogen bond [20]. According to the above reasoning an important difference between β-sheet and α-helix folding is that nucleation of the former structure should be more disfavored entropically whereas its elongation should be more favored enthalpically. Which of the two structural motifs prevails is determined by the sequence of amino acid residues. This is a thermodynamic argument in complete agreement with models [21] of protein structure that consider the global energy minimum as the state occupied by the native structure.

The same α-helix$-\beta$-sheet balancing is important here, since the present problem may be seen as an α-helix $\leftrightarrow$ β-strand $\leftrightarrow$ β-sheet $\rightarrow$ amyloid equilibrium where the last stage is non-reversible. The fact that β-sheet folding is intermolecular suggests that it may be rendered non-cooperative if the nascent β-strand is stabilized by intramolecular interactions. This problem will be examined in detail in the following sections.

3. Methods

Five main chain rotamers (A: $\phi = -57$, $\psi = -47$; B: $\phi = -139$, $\psi = 135$; G: $\phi = -60$, $\psi = -30$, D: $\phi = -90$, $\psi = 0$ and E: $\phi = 70$, $\psi = -60$) were employed in the conformational search. For the side chain conformations we have made use of the gauche minus, trans and gauche plus rotamers of the Ponder and Richards classification [22] (the numerals 1, 2 and 3 indicate, respectively, the gauche minus, trans and gauche plus rotamers of χ_1). Gas phase energies were calculated with the ECEPP/2 force field [23]. Hydration free energies were calculated with the Ooi et al. [24] hydration potentials and the Connoly routine [25] for surface area computation. Matrix operations described in the literature [12] were employed in the conformational search. Probabilities of occurrence of chain conformations were calculated with a partition function formed by the states obtained in the conformational search. To create the model of amyloid fibrils monomer templates described below were oriented in order to form parallel and antiparallel β-sheets and submitted to 10 000 steps of a non-constrained geometry energy minimization with the CVFF forcefield [26] and the steepest descents algorithm by using the Discover software furnished by Molecular Simulations.

4. Results and discussion

4.1. A model of amyloid fibrils

Despite the absence of sequence homology between the peptide chains listed in Table 1 and synthetic models [9] of α/β transitions (such as the sequence AEAEAKAKAEAEAKAK derived from the DNA binding zuotin protein [27]) there is one important feature that they have in common. Namely, a periodicity that, when the α-heli-

Table 1
Polypeptide chains part of the present conformational search. Peptide chains in the study and the corresponding five most stable conformations for which part of the chain is a β-strand

(i)		(ii)		(iii)	
GAAAAGAVVGGLGGYM[a]		GAAAAGAVVGGLGGYMLGSA		KTNMKHMAGAAAAGAVVGGLG	
DBBBBGBAGAAAAAGD[b]		DBBBBGBAAAAAAABDGGAGD		EBAABDBBBBBGBDBGAAGDD	
1111111131111121	0.30022E-03[c]	1111111111111121121	0.16132E-09	11111321111111121111	0.26770E-08
BDABBBBGGAAAAAGD		DBBBBGBAAAAAABDGGAAD		GBGBDBBBBBBGBDBGAAGDG	
1111111331111121	0.64792E-05	1111111111111121121	0.15749E-09	32113221111111121111	0.26016E-08
BDGBBBBGGAAAAAGD		DBBBBGBAAAAAAABDGGAGD		DDDDBDBBBBBGBDBGAAGDD	
1111111331111121	0.64645E-05	1111111111111121111	0.15718E-09	21111221111111121111	0.24937E-08
BBBBDBBGGAAAAAGD		DBBBBGBAAAAAABDGGAAD		DBDDBDBBBBBGBDBGAAGDG	
1111111331111121	0.64517E-05	1111111111111121111	0.13011E-09	32111111111111121111	0.24897E-08
GBBBBABGGAAAAAGD		DBBBBGBAAAAAABDGGAGD		AGABDBBBBBBGBDBGAAGDG	
1111111131111121	0.57612E-05	1111111111111121131	0.89692E-10	21112221111111121111	0.24858E-08

[a] Sequence of amino acid residues.
[b] Letter and numerals indicate, respectively, main chain and side chain rotamers as defined in Section 3.
[c] Probability of occurrence calculated as shown in Section 3, for an absolute temperature of 500 K.

cal conformation is adopted, enables [28] the formation of $(i, i + 4)$ ionic bonds and, in the former case, van der Waals contacts that bury the hydrophobic surfaces of amino acid side chains.

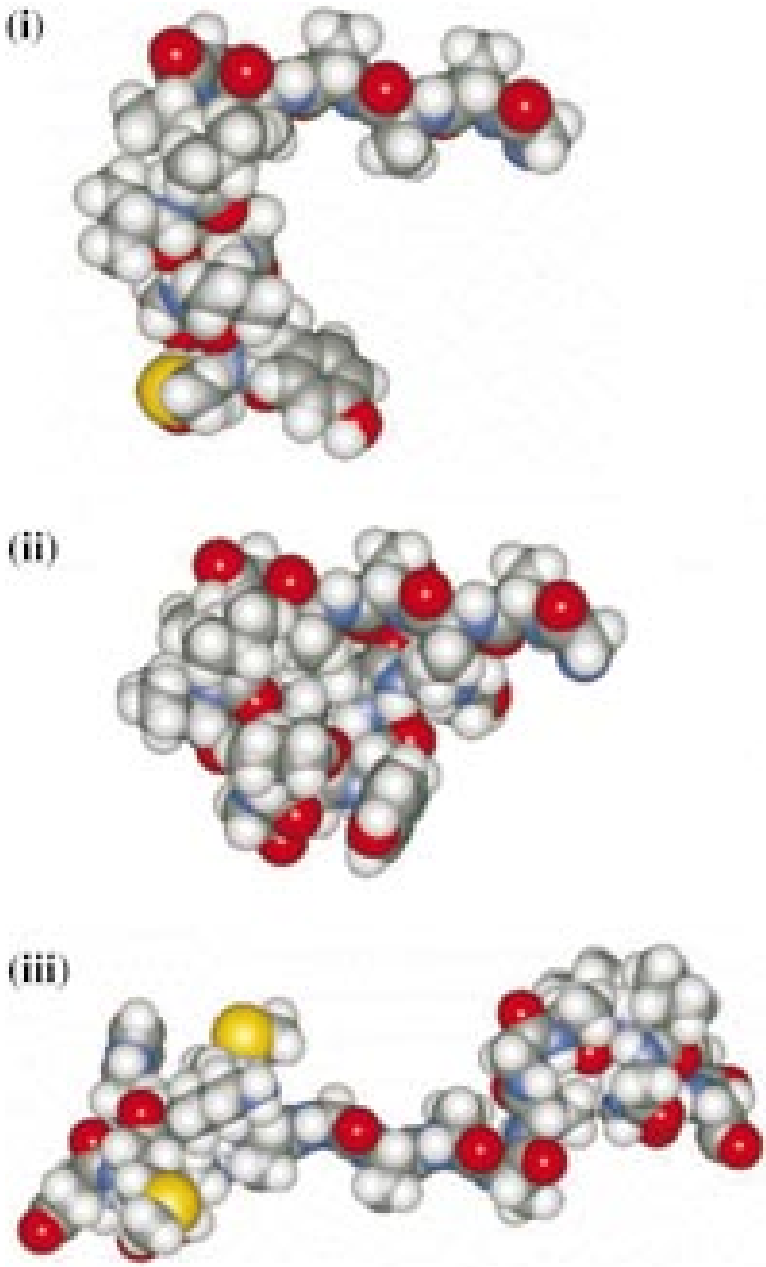

Fig. 1. The most stable β-strand conformations found in the conformational search to be adopted by the peptide chains listed in Table 1: (i) DBBBBGBAGAAAAAGD (111111131111121) chain conformation of peptide i. (ii) DBBBBGBAAAAAABDGGAGD (11111111111111121121) chain conformation of peptide ii. (iii) EBAABDBBBBBGBDBGAAGDD (111113211111111121111) chain conformation of peptide iii. Letters and numerals indicate, respectively, main chain and side chain rotamers as defined in Section 3. Color coding: white, hydrogen; black, carbon; blue, nitrogen; red, oxygen; yellow, sulfur.

Indeed, as shown in the conformations depicted in Fig. 1 the separation between valine, leucine, and methionine side chains is ideal for the formation of van der Waals contacts.

It has also been shown [9] for the mentioned synthetic models of amyloid that this same sequence periodicity also enables the formation of intermolecular contacts that contribute to the stabilization of a β-sheet. This analogy suggests that a sequence periodicity that contributes to the stabilization of both the α-helical and the β-sheet conformations is part of the mechanism by which amyloid plaques are formed. The following analysis shows, however, that other factors may be equally important.

To examine the question of whether the formation of amyloid is a cooperative process, a conformational analysis of the peptide chains listed in Table 1 was carried out according to Eq. (1) and Eq. (2). The resulting sets of conformations were screened for α-helix/β-strand transitions. Part of the results obtained for the peptide chains (i), (ii) and (iii) is shown in Table 1. In agreement with the above discussion, occurrence of the α-helical conformation was found to be predominant near the carboxy end where it contributes to the stabilization of the hydrophobic cluster VVGGLGGYM (VVGGLG in the case of peptide (iii)), as shown in the various structures depicted in Fig. 1.

It is also shown in Fig. 1 that according to our calculations peptides (i) and (ii) have a tendency for the adoption of two structural domains which are an α-helical region in the carboxy end domain and a β-strand conformation in the amino end domain. Peptide (iii) shows a tendency to adopt two globular and one extended domain. This is an unusual feature which, as far as we know, is absent from the set of known protein structures. Unlike the stabilization of a single β-strand by interactions with the remaining part of the chain shown in Fig. 1, in globular proteins β-strands are stabilized by being part of β-sheets.

An important consequence of the above discussion is that, for those conformations which similarly to the structures displayed in Fig. 1 have a segregated β-strand, seeding of β-sheet clusters should be a non-cooperative process, since in this case the entropy loss due to the freezing of β-strand main chain dihedrals is absent from the nucleation stage. This should be an important difference between formation of β-sheet in amyloid plaques and the same process in protein structures.

A mechanistic explanation for the amyloidogenic action of peptides (i)–(iii) is strongly suggested by the structures depicted in Fig. 1, where the occurrence of extended and coiled structural domains is clearly seen. Assuming that the neurotoxic action of these peptides is to promote the formation of β-sheet aggregates, it is a natural choice to attribute to the extended domain the role of binding to available β-sheet regions. As to the coiled domain, we tentatively attribute to it the role of promoting α-helix to β-sheet transi-

Table 2
Hydration free energies (kcal/mol) of the amino acid residues belonging to the peptides listed in Table 1 when adopting the conformations shown in Fig. 1

	(i)	(ii)	(iii)
K			−5.054
T			−1.214
N			−0.712
M			−0.397
K			−2.044
H			−3.191
M			−0.223
A			0.820
G	−1.229	−1.229	0.693
A	0.503	0.598	0.321
A	0.318	0.271	−0.160
A	0.262	0.637	−1.067
A	−0.290	−0.395	−0.264
G	−0.601	−0.714	0.348
A	−0.249	−0.424	0.784
V	2.094	0.039	−0.041
V	0.144	1.107	0.128
G	0.675	−0.191	0.070
G	1.379	1.010	0.073
L	1.118	0.842	0.857
G	0.603	0.658	3.598
G	0.432	−0.013	
Y	−3.672	−2.197	
M	2.235	−0.312	
L		0.208	
G		0.239	
S		−1.723	
A		1.488	

tions as it partially unfolds to form an extended chain conformation.

According to this model the β-sheet region of amyloid plaques is also a hydrophobic core. In Table 2 are shown the amino acid residue hydration energies corresponding to the structures depicted in Fig. 1. A comparison between Tables 1 and 2 shows that the β-strand domains seen in Fig. 1 are coincident with hydrophobic regions.

Additional information is provided by the energy distributions of α-helical and β-strand conformations shown in Fig. 2. For the neurotoxic peptide (i) the first maxima of the β-strand energy distribution is 7 kcal/mol above the energy minimum (found in the present conformational search). For peptides (ii) and (iii) this energy difference is 20 and 19 kcal/mol, respectively, corresponding to the very low probabilities of occurrence shown in Table 1.

Based on the above described conformational analysis of the amyloidogenic peptides listed in Table 1, we have built molecular models of clusters formed by peptide (iii). The chain conformation depicted in Fig. 1(iii) was chosen as the building block of the models of amyloid fibrils represented in Figs. 3 and 4.

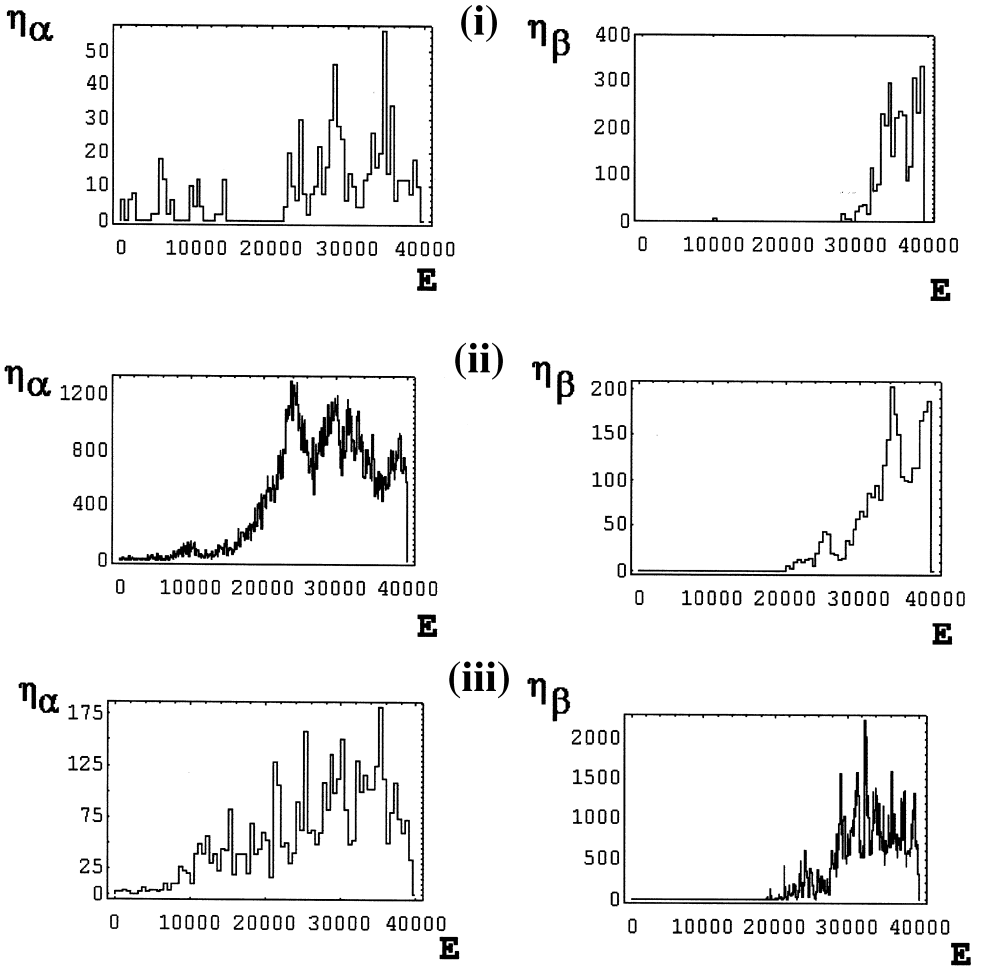

Fig. 2. Density of states vs. energy plots showing for the polypeptide chains listed in Table 1 the energy distributions of α-helix and β-strand conformations. η_α and η_β are, respectively, the densities of α-helix and β-strand states. E is the internal potential energy in cal/mol rescaled so that the least energy conformation is the zero energy level.

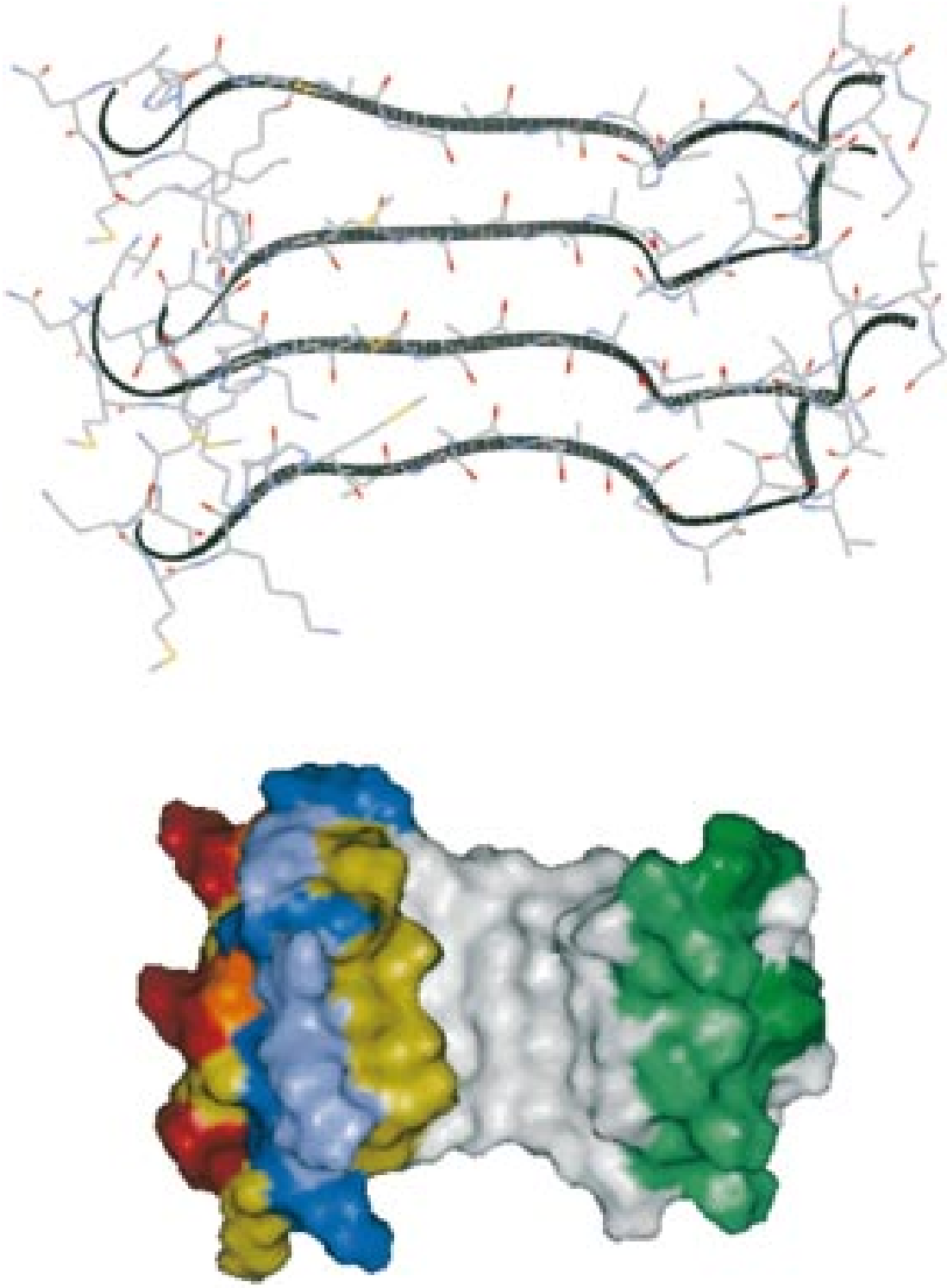

Fig. 3.

It is assumed that intermolecular interactions involving peptide (iii) chains direct the formation of β-sheet aggregates. The association of Met7-Gly8-Ala9-Ala10-Ala11 β-strand segments which are part of structure 1(iii) determines the axial register of adjacent chains. There are four parallel and four antiparallel β-sheet orientations. In each case, there are two orientations in which in register amino and carboxy and globular domains point to opposite directions (data not shown) and two orientations that cause a partial interfacing of globular domains.

Since it is our purpose to describe close packed clusters only the latter orientations were, in principle, considered. An examination of the corresponding molecular models showed that one of these two parallel orientations creates unfavorable Lys1-Lys1, Lys5-Lys5 and His6-His6 electrostatic pairs by placing the corresponding side chains in close contact and that an antiparallel orientation results in several conflicting overlaps between Met4-Ala8 and Ala11-Val16 chain segments. By excluding these orientations we ended with one parallel and one antiparallel model of amyloid aggregation. A non-constrained geometry energy minimization (see Section 3 for details) was then applied to each model resulting in β-sheets formed by β-strands twisted to nearest neighbors by an average of 10°.

From a molecular mechanics standpoint, the parallel orientation is more stable by 15 kcal/mol mainly due to non-bonded interactions. Since, as shown in Table 2, the amino end of the peptide conformation depicted in Fig. 1(iii) is hydrophilic whereas the remaining part of the chain is hydrophobic, the two orientations also differ with respect to the hydrophobicity of intermolecular intrasheet interactions. As shown in Fig. 3 in the parallel orientation the alignment of Met 7 side chains (yellow surface) and Val16, Val17 and Leu20 side chains (green surface) causes an extensive accretion of hydrophobic surface. On the other hand, in the antiparallel orientation represented in Fig. 4, Met4 and Val16, Val17 and Leu20 are part of hydrophobic clusters. In both orientations the packing of chain fragments formed by Met7 and Ala8-Ala15 (white surface) creates a hydrophobic core.

The main features of these models are: the inner hydrophobic core; despite the high β-sheet content the structure is only partially a β-sheet; fibril growth along an axis perpendicular to the β-sheet; high regularity and symmetry considered to be in accordance with limited regions of amyloid fibrils.

5. Conclusion

X-ray diffraction measurements [29,30] have shown the existence of β-sheets extended along the length of the amyloid fibrils. A similar packing would result if the amyloid-forming protein had, as has been shown [11], one or more regions with a propensity for α/β transitions, since β-strand segments would be aligned in the fibril. The peptides of Table 1 also undergo α/β transitions in different chain regions although the possibilities are much more limited than in a protein chain. Moreover, in Figs. 3 and 4 β-strands are aligned perpendicularly to the long axis of the fibril forming a twisted β-sheet, in accordance with X-ray [29,30] data.

The experimental facts [31] and the present calculations have shown that the PrP^c segment 106–126 adopts both the α-helix and the β-strand conformations. Also consistent with the experimental data is the fact that in the structures depicted in Fig. 1 the β-strand comprehends the chain segment GAAAAG, since the octapeptide AGAAAAGA is sufficient [10] for amyloid formation.

We have shown that the intervention of low probability β-strands whose distinguishing features are non-participation in intramolecular β-

Fig. 3. Wire frame model and solvation surface of an amyloid cluster formed by the parallel orientation of four peptide iii chains listed in Table 1 adopting the conformation represented in Fig. 1(iii). Color coding: wire frame: white, hydrogen; black, carbon; blue, nitrogen; red, oxygen; yellow, sulfur; line ribbon: black; hydration surface: white, glycine and alanine; green, valine and leucine; yellow, sulfur; blue, lysine, histidine; red, threonine; brown, asparagine.

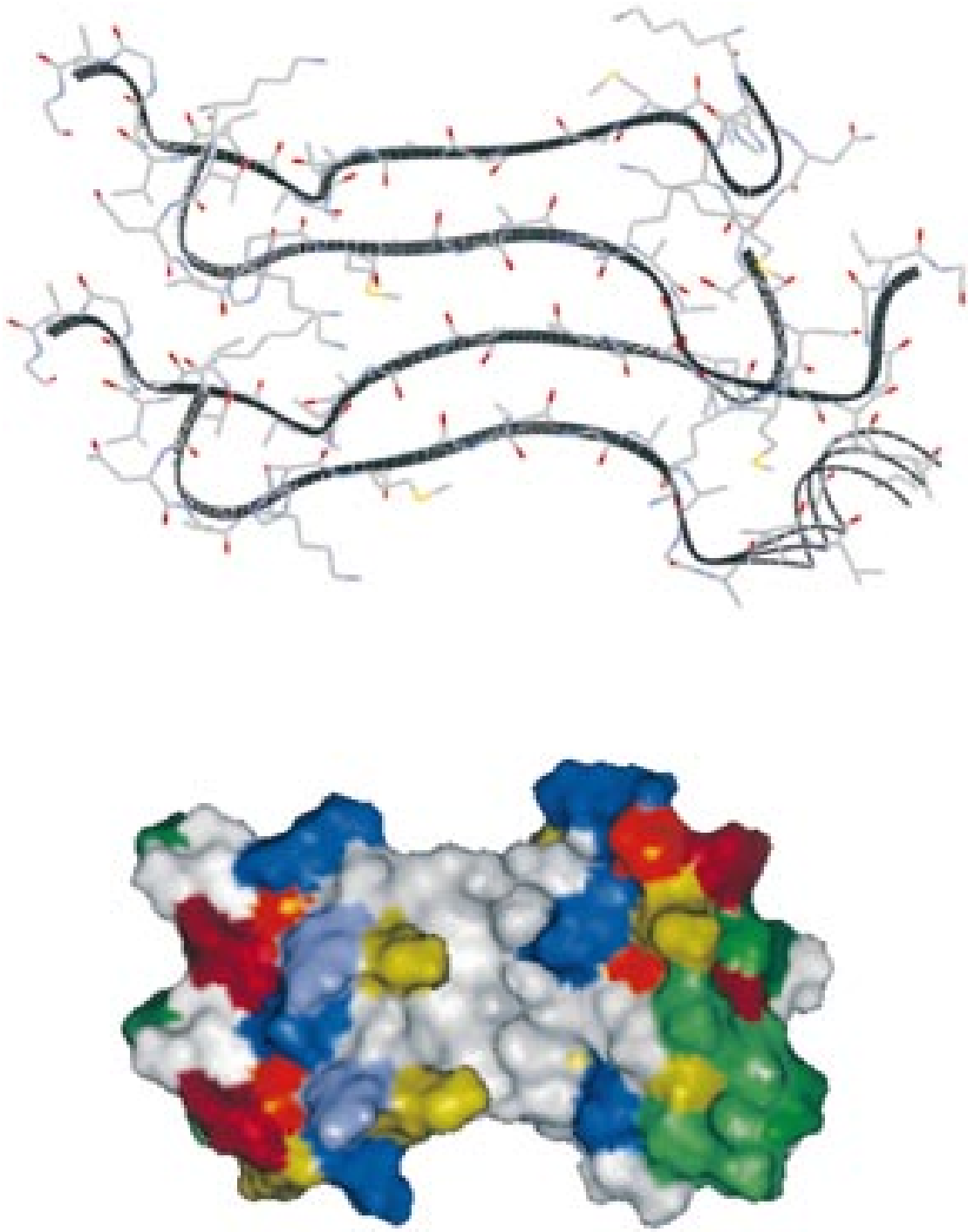

Fig. 4. Wire frame model and solvation surface of an amyloid cluster formed by the antiparallel orientation of four peptide iii chains listed in Table 1 adopting the conformation represented in Fig. 1(iii). Color coding: wire frame: white, hydrogen; black, carbon; blue, nitrogen; red, oxygen; yellow, sulfur; line ribbon, black; hydration surface: white, glycine and alanine; green, valine and leucine; yellow, sulfur; blue, lysine, histidine; red, threonine; brown, asparagine.

sheets, hydrophobicity and stabilization by intramolecular interactions may be instrumental in the formation of amyloid fibrils.

Intramolecular stabilization compensates the entropy loss associated with the formation of β-strands that subsequently engage in non-bonded and hydrophobic self-associating interactions. As a consequence, non-similar mechanisms of β-sheet folding take place in proteins and amyloid fibrils.

Since there is a partial homology between peptides (i)–(iii) and the amyloid β-peptide [32], we expect an ongoing study of amyloid β fibrils to yield similar conclusions. We are also interested in knowing whether the described β-strands may interact with other proteins.

Recently, the PrP^{C} structure of the infectious PrP^{SC} fragment was determined [33] showing that the 23-residue N-terminal region containing the peptide chains, part of the present study, is largely disordered. There is also substantial evidence [10,11,31,32] that peptide fragments belonging to this region undergo α/β transitions and intermolecular association. The present results suggest that low probability N-terminal PrP^{SC} hydrophobic β-strands play a role in pathogenic activity. A related problem is whether the prion protein receptor, recently shown [34] to bind peptide (i), also results in a β-strand.

Acknowledgements

We are grateful to the NCI's Laboratory of Mathematical Biology in Bethesda, MD, USA and to the Crystallography Group of the University of Sao Paulo in Sao Carlos, SP, Brasil for the use of computer facilities and support provided by staff personnel. This work was supported by FAPESP.

References

[1] T.E. Creighton, Proteins, W.H. Freeman, New York, 1984.
[2] P. Keh-Ming, M. Baldwin, J. Nguyen, M. Gasset, A. Serban, D. Groth, I. Mehlhorn, Z. Huang, R.J. Fletterick, F.E. Cohen, S.B. Prusiner, Proc. Natl. Acad. Sci. USA 90 (1993) 10962.
[3] B.T. Hyman, J.J. Werniger, R.E. Tanzi, Mol. Brain. Res. 18 (1993) 253.
[4] J.T. Jarret, P.T. Lansbury, Jr., Cell 73 (1993) 1055.
[5] S.B. Prusiner, Trends Biochem. Sci. 21 (1996) 482.
[6] G.C. Glenner, C.W. Wong, Biochem. Biophys. Res. Commun. 120 (1984) 885.
[7] D.R. Booth, M. Sunde, V. Bellotti, C.V. Robinson, W.L. Hutchinson, P.E. Fraser, P.N. Hawkins, C.M. Dobson, S.E. Radford, C.C.F. Blake, M.B. Pepys, Nature 385 (1997) 787.
[8] G. Goldstein, K. Andersson, A. Olofsson, I. Dacklin, A. Edvinsson, V. Baranov, O. Sandgren, C. Thylen, S. Hammarstrom, E. Lundgren, Biochemistry 36 (1997) 5346.
[9] S. Zhang, C. Lockshin, R. Cook, A. Rich, Biopolymers 34 (1994) 663.
[10] M. Gasset, M.A. Baldwin, D.H. Lloyd, J.M. Gabriel, D.M. Holtzman, F. Cohen, R. Fletterick, S.B. Prusiner, Proc. Natl. Acad. Sci. USA 89 (1992) 10940.
[11] G. Forloni, N. Angaretti, R. Chiesa, E. Monzani, M. Salmona, O. Bugiani, F. Tagliavini, Nature 362 (1993) 543.
[12] S.G. Jacchieriand, R.L. Jernigan, Biopolymers 32 (1992) 1342.
[13] S.G. Jacchieri, A. Ito, Int. J. Quant. Chem. 53 (1995) 335.
[14] S.G. Jacchieri, M.D. Gomes, L. Juliano, A.C.M. Camargo, J. Pept. Res. 51 (1998) 452.
[15] A. Sali, E. Shakhnovich, M. Karplus, J. Mol. Biol. 235 (1994) 1614.
[16] S.G. Jacchieri, Int. J. Quant. Chem. 65 (1997) 1115.
[17] M. Vasquez, H.A. Scheraga, Biopolymers 24 (1985) 1437.
[18] S.G. Jacchieri, M. Gomes, A.C.M. Camargo, L. Juliano, Int. J. Quant. Chem. 23 (1996) 1815.
[19] S.G. Jacchieri, N.G.J. Richards, Biopolymers 33 (1992) 325.
[20] C. Cantor, P.R. Schimmel, Biophysical Chemistry, W.H. Freeman, New York, 1980.
[21] H.A. Scheraga, Biophys. Chem. 59 (1996) 329.
[22] J.W. Ponder, F.M. Richards, J. Mol. Biol. 193 (1987) 775.
[23] K. Gibson, H.A. Scheraga, J. Comput. Chem. 8 (1987) 826.
[24] T. Ooi, M. Oobatake, G. Nemethy, H.A. Scheraga, Proc. Natl. Acad. Sci. USA 84 (1987) 3080.
[25] M.L. Connoly, J. Appl. Cryst. 16 (1983) 548.
[26] P. Dauber-Osgutorphe, V.A. Roberts, D.J. Osguthorpe, J. Wolff, M. Genest, Prot. Struct. Funct. Genet. 4 (1988) 31.
[27] S. Zhang, C. Lockshin, A. Herbert, E. Winter, A. Rich, EMBO J. 11 (1992) 3787.
[28] G. Merutka, W. Lipton, W. Shalongo, P. Sooh-Ho, E. Stellwagen, Biochemistry 29 (1990) 7511.
[29] C.C.F. Blake, L.C. Serpell, M. Sunde, O. Sandgren, E. Lundgren, in: The Nature and Origin of Amyloid Fibrils, John Wiley, Chichester, 1996, p. 6.

[30] C.F. Blake, L.C. Serpell, Structure 4 (1996) 989.
[31] L. De Gioia, C. Selvaggini, E. Ghibaudi, L. Diomede, O. Bugiani, G. Forloni, F. Tagliavini, M. Salmona, J. Biol. Chem. 269 (1994) 7859.
[32] J.H. Come, P.E. Fraser, P.T. Lansbury, Jr., Proc. Natl. Acad. Sci. USA 90 (1993) 5959.
[33] T.L. James, H. Liu, N.B. Ulyanov, S. Farr-Jones, H. Zhang, D.G. Donne, K. Kaneko, D. Groth, I. Mehlhorn, S.B. Prusiner, F.E. Cohen, Proc. Natl. Acad. Sci. USA 94 (1997) 10086.
[34] V.R. Martins, E. Graner, J. Garcia-Abreu, S.J. Souza, A.F. Mercadante, S.S. Veiga, S.M. Zanata, V. Moura Neto, R. Brentani, Nature Med. 3 (1997) 1376.